UNIVERSITY of
BRADFORD

Library

The University of Bradford Institutional Repository

http://bradscholars.brad.ac.uk

Link to publisher's version: *http://doi.org/10.1016/j.advengsoft.2016.02.007*

Citation: Golafshani EM and Ashour AF (2016) A Feasibility Study of BBP for predicting shear capacity of FRP reinforced concrete beams without stirrups. Advances in Engineering Software. 97: 29-39.

A Feasibility Study of BBP for predicting shear capacity of FRP reinforced concrete beams without stirrups

Emadaldin Mohammadi Golafshani[a*], Ashraf Ashour[b]

[a] Department of Civil Engineering, Tehran Science and Research Branch, Islamic Azad University, Tehran, Iran
[b] School of Engineering, Design and Technology, University of Bradford, Bradford BD7 1DP, UK

Abstract

Shear failure of concrete elements reinforced with Fiber Reinforced Polymer (FRP) bars is generally brittle, requiring accurate predictions to avoid it. In the last decade, a variety of artificial intelligence based approaches have been successfully applied to predict the shear capacity of FRP Reinforced Concrete (FRP-RC). In this paper, a new approach, namely, biogeography-based programming (BBP) is introduced for predicting the shear capacity of FRP-RC beams based on test results available in the literature. The performance of the BBP model is compared with several shear design equations, two previously developed artificial intelligence models and experimental results. It was found that the proposed model provides the most accurate results in calculating the shear capacity of FRP-RC beams among the considered shear capacity models. The proposed BBP model can also correctly predict the trend of different influencing variables on the shear capacity of FRP-RC beams.

Keywords: Shear capacity; FRP reinforced concrete; Biogeography-based programming; Evolutionary Computation.

1. Introduction

The deterioration of reinforced concrete (RC) structures due to corrosion of steel reinforcement has become a serious and costly problem in recent decades [1-5, 8, 9]. In order to avoid such problem, the use of fiber reinforced polymer (FRP) bars as internal longitudinal flexural reinforcement has emerged as an alternative solution for structural members subjected to severe environmental exposure [4,8,10]. FRPs are non-corrodible materials with the potential of reducing life-cycle costs in applications where corrosion of steel reinforcements causes costly maintenance. The use of FRP bars, however, is not only limited to cases where corrosion is the main concern. FRP bars have remarkable properties, such as durability, high strength to weight ratio, non-magnetism and good fatigue properties making them attractive as reinforcement for RC structures [5, 11]. They are most common in applications such as parking garages and bridge decks subject to severe corrosion from deicing salts, or in hospital magnetic resonance imaging (MRI) units where non-ferromagnetic systems are required. They have also been introduced in integrally insulated sandwich walls where low thermal conductivity is desired [12].

Direct substitution of steel reinforcement with FRP materials is not possible without consideration of their structural performance [9]. Shear failure in RC beams is one of the most undesirable modes of failure due to its rapid progression. Consequently, for safe design, a number of guidelines and standards provide methods for shear design of FRP-RC members [13]. It is commonly accepted that the shear transfer in RC elements without transverse reinforcement is composed of several shear mechanisms including shear resisted by un-cracked concrete compressive zone, friction forces developed along the concrete crack length (aggregate interlock) and shear from dowel action of longitudinal reinforcement. The relative contribution of each mechanism changes as the load increases. In the case of FRP-RC beams without stirrups, FRP modulus of elasticity is significantly lower than that of steel bars. Consequently, crack

widths are larger and shear stiffness of FRP reinforcement is lower, thus reducing both aggregate interlock and dowel action mechanisms [10].

Several artificial intelligence (AI) methods are increasingly used as alternatives to more classical or conventional techniques. AI techniques have been used to solve complicated, practical problems in different sectors, such as engineering, economics, medicine, military, marine, etc., and are becoming more popular nowadays [14]. Symbolic regression (SR) is a relatively new branch of AI. It is a process of evolving summary expressions for available data by analyzing and modeling numerical multivariate data sets, when some data of unknown process are obtained. Unlike traditional linear and nonlinear regression methods that fit parameters to an equation of a given form, SR tries to form mathematical equations by searching the parameters and the form of equations [15, 16]. In other words, SR searches nonlinear equation form and its parameters simultaneously for an addressed modeling problem. It attempts to derive a mathematical function to describe the relation between dependent and independent variables. The problem of SR is an optimization problem the purpose of which is finding the best combination of variables, symbols, and coefficients to develop an optimum model satisfying a set of fitness cases [16]. Depending on the type of optimization strategy applied for SR, different branches of SR have been introduced, such as Genetic programming (GP) [17], Immune programming (IP) [18], Dynamic ant programming (DAP) [19], Clone selection programming (CSP) [20] and artificial bee colony programming (ABCP) [16]. Various types of GP have been applied successfully in different areas of civil engineering. However, IP, DAP, CSP and ABCP are new branches of SR that need to be applied to a variety of real world problems and their performance should be investigated.

Biogeography-Based Optimization (BBO) is one of the recent metaheuristic algorithms proposed by Simon, which is inspired by the geographical distribution and migration of species in an ecosystem [21]. In recent years, BBO has been comprehensively developed to the extent that it performs better than other widely used heuristic algorithms like genetic algorithms, ant colony optimization, particle swarm optimization, differential evolution, and simulated annealing for some well-known benchmarks [22-24]. BBO has successfully applied to several practical problems, such as sensor selection problems for aircraft engine health diagnostics [21], groundwater possibility retrieval systems [25] and power flow problems [26].

In this paper, Biogeography-Based Programming (BBP), inspired by BBO, is proposed as a new type of machine learning method for SR for predicting the shear capacity of FRP-RC beams. Moreover, a qualitative analysis of the influencing parameters using the proposed model is also carried out. The rest of this paper is organized as follows: Section 2 presents a literature review on different equations of several building codes and various AI methods for simulating the shear capacity of FRP-RC beams. Section 3 describes basic concepts of BBO, Section 4 introduces the proposed BBP model as a new machine learning approach. Section 5 describes the data and the parameter settings used in this work. In section 6, the analysis of the results and the sensitivity analysis are presented, whereas Section 7 summarizes the main conclusions and achievements of the investigation.

2. Overview of shear capacity prediction models of FRP-RC beams

Because of the rapid increase of using FRP materials as internal reinforcement for concrete structures, there are international efforts to develop design guidelines. Therefore, several design equations have been proposed for predicting the shear capacity of FRP-RC beams without stirrups with varying success. These design equations address the unique characteristics of FRP reinforcement affecting the shear behavior of flexural members. Most of the shear design equations incorporated in these codes and guidelines have focused on modifying existing shear design equations for steel-RC beams to account for the substantial differences between FRP and steel reinforcement. For example, JSCE [27], BISE [28], CNR DT 203/2006 [29], ISIS-M03-07 [30], Tottori and Wakui [31] apply a correction factor E_f/E_s that takes into account the difference in the elastic moduli between FRP, E_f, and steel reinforcement, E_s. However, this modification factor E_f/E_s is raised to different powers in these guidelines [32]. On the other hand, the modification proposed by ACI-440.1R-06 [33], CAN/ CSA-S806-02 [34], Razaqpur and Isgor [35] and El-Sayed et al. [36] only includes the FRP reinforcement axial rigidity E_fA_f. Some of the shear design equations for shear capacity of FRP-RC beams are summarized in Table 1. Note that all strength reduction design factors used in these shear design equations are set equal to one for comparison purposes.

Few researchers have applied several AI methods for predicting the shear capacity of FRP-RC beams. Kara [37] presented a simple improved model to calculate the concrete shear capacity of FRP-RC slender beams without stirrups based on the gene expression programming (GEP) approach. Bashir and Ashour [32] investigated the feasibility of using artificial neural networks (ANNs) to predict the shear capacity of FRP-RC beams without any shear reinforcement. Nasrollahzadeh and Basiri [38] developed an AI-based method using fuzzy inference system (FIS) to predict the shear capacity of FRP-RC beams. Lee and Lee [39] presented a theoretical model based on an artificial neural network (ANN) for predicting the shear capacity of slender FRP-RC flexural members without stirrups. All the above mentioned investigations concluded that their proposed models could predict to a high level of accuracy the shear capacity of FRP-RC beams without any shear reinforcement.

Table 1
Summary of the shear design formulations used in this paper.

Shear procedure	Equations/variables
ACI440.1R-06 [33]	$v_{cf} = \dfrac{2}{5}\sqrt{f_c'}\,b_w d\left(\sqrt{2\rho_f n_f + (\rho_f n_f)^2} - \rho_f n_f\right)$ $n_f = \dfrac{E_f}{E_c}$
CAN.CSA S806-02 [34]	$v_{cf} = 0.035\lambda b_w d\left(f_c'\rho_f E_f \dfrac{v_f d}{M_f}\right)^{1/3}\quad d \leq 300\ mm$ $\dfrac{v_f d}{M_f} \leq 1\ and\ 0.1\lambda b_w d\sqrt{f_c'} \leq v_{cf} \leq 0.2\lambda b_w d\sqrt{f_c'}$ $v_{cf} = \dfrac{130}{1000+d}\lambda b_w d\sqrt{f_c'},\quad d > 300\ mm$ $v_{cf} \geq 0.08\lambda b_w d\sqrt{f_c'}$
ISIS M03-07 [30]	$v_{cf} = 0.2\lambda b_w d\sqrt{f_c'\dfrac{E_f}{E_s}},\qquad d \leq 300\ mm$ $v_{cf} = \dfrac{260}{1000+d}\lambda b_w d\sqrt{f_c'\dfrac{E_f}{E_s}},\qquad d > 300\ mm$ $v_{cf} \geq 0.1\lambda b_w d\sqrt{f_c'\dfrac{E_f}{E_s}}$
JSCE-97 [27]	$v_{cf} = \beta_d\beta_p\beta_n f_{vcd} b_w d$ $\beta_p = \sqrt[3]{\dfrac{100\rho_f E_f}{E_s}} \leq 1.5$ $\beta_d = \sqrt[4]{\dfrac{1000}{d}} \leq 1.5$ $\beta_n = 1.0\ (in\ case\ of\ no\ axial\ force)$ $f_{vcd} = 0.2\sqrt[3]{f_c'} \leq 0.72\ (MPa)$
CNR-DT 203/2006 [29]	$v_{cf} = 1.3\left(\dfrac{E_f}{E_s}\right)^{\frac{1}{2}}(\tau_{rd}k_d(1.2 + 40\rho_f)b_w d)$ $\tau_{rd} = 0.25 f_{ctk,0.05}$ $k_d = 1.6 - d \geq 1$ $1.3\left(\dfrac{E_f}{E_s}\right)^{\frac{1}{2}} \leq 1$
BISE-99 [28]	$v_{cf} = 0.79\left(100\rho_f\dfrac{E_f}{E_s}\right)^{\frac{1}{3}}(\dfrac{400}{d})^{0.25}(\dfrac{f_{cu}}{25})^{1/3}b_w d$ $\dfrac{400}{d} \leq 1$

Note: v_{cf}: shear capacity; f_c': concrete compressive strength; b_w and d: beam's width and effective depth, respectively; ρ_f: longitudinal reinforcement ratio, E_c, E_s and E_f: elastic modulus of concrete, steel and longitudinal bars, respectively; M_f and V_f: moment and shear force at critical section, respectively; β_n: factor of axial force, respectively; λ: concrete density factor; f_{cu}: cube compressive strength of concrete ($1.25 f_c'$); $f_{ctk,0.05}$: characteristic concrete tensile strength (5% fractile).

3. Biogeography- Based Optimization (BBO)

Biogeography science is defined as the study of the distribution of species and ecosystems over the surface of the earth, in both space and time [40-43]. The distribution of species across the surface of the earth usually depends on a combination of environmental reasons. In the natural world, species tend to explore more suitable environments. A good habitat, tend to have a large number of species, has a high suitability index (HSI) and vice versa. During the progress of evolution, habitats with a high HSI have a low species immigration rate because they are already nearly saturated with species. Over time, the habitats with high HSI will have more species, while those with low HIS come to have fewer. Inspired by this idea, Dan Simon [21] proposed a new evolutionary algorithm named Biogeography-Based Optimization (BBO). Mathematically speaking, a habitat presents a possible solution for the optimization problem. BBO utilizes mathematical models to describe the biogeographical behavior using migration, mutation and the distribution of species [43]. In the following, the main components of BBO are explained.

Migration is a probabilistic operator. The migration rates of each solution are used to modify existing solution by sharing features within the population. For each feature of a given solution y_k, the immigration rate λ_k of y_k determines the probability of immigration of current solution. If the solution y_k is selected for immigration, then the emigrating solution y_j is probabilistically chosen based on the emigration rate μ_j. Migration is written as [44]:

$$y_k(s) \leftarrow y_j(s)$$

where s is a solution feature. Immigration and emigration rates are functions of the number of species in the habitat, such as the linear migration curves in Fig. 1.

Mutation is a probabilistic operator that randomly modifies a solution feature. The purpose of mutation is to enhance the diversity of the population which helps to decrease the chances of getting trapped in local optima [44].
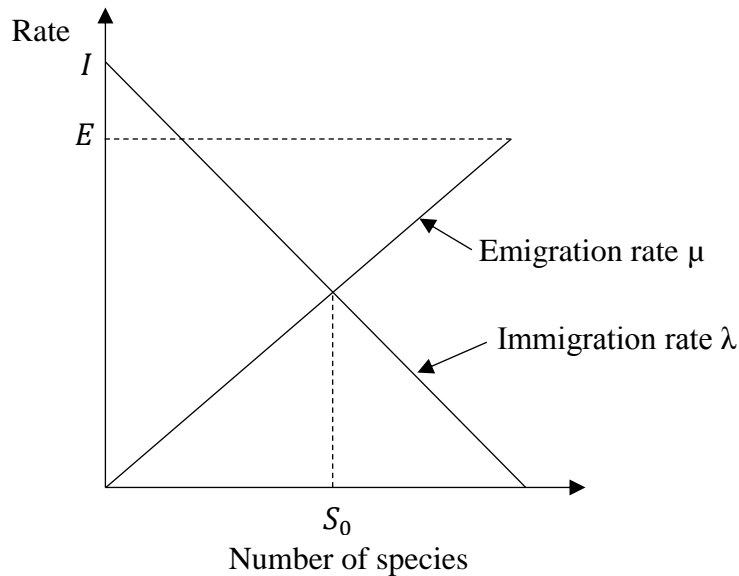

Fig. 1. The relationship between the number of species and the migration rates [21].

4. Biogeography- Based Programming (BBP)

Similar to other automatic programming algorithms, the proposed BBP aims at developing to a mathematical expression. This, basically, is an explicit relation between one or more inputs and an output using mathematical "symbols" functions, variables and constants. The process of programming is a subset of symbolic function identification and it differs from conventional regression in that it does not calculate the coefficients/functions. The way it finds equations is by carrying out an extensive, continuously improving guided search in an evolving search space.

The proposed BBP continues the trend of dealing with the problem of representation in BBO by increasing the complexity of the structures undergoing adaptation. In particular, the structures undergoing adaptation in BBP are general, hierarchical computer programs of dynamically varying size and shape. The proposed BBP is based on mathematical models of biogeography describing natural ways of distributing species, i.e., how species migrate, how they arise and become extinct. The BBP serves to provide a platform with operators such as random generation, mutation and migration that produce, alter and select habitats in population. This is facilitated by storing expression in tree data structures in the computer memory. Tree structures are easy to swap parts of the program and append or remove parts, which are operations carried out by habitation operators. A habitat consists of one or more sub-habitats and the performance of sub-habitats determines the efficiency of the corresponding habitat. Each sub-habitat has mathematically an expression tree and the aggregation of sub-habitats constitute a habitat. Fig. 2 illustrates tree structure of a sub-habitat and the corresponding habitat.
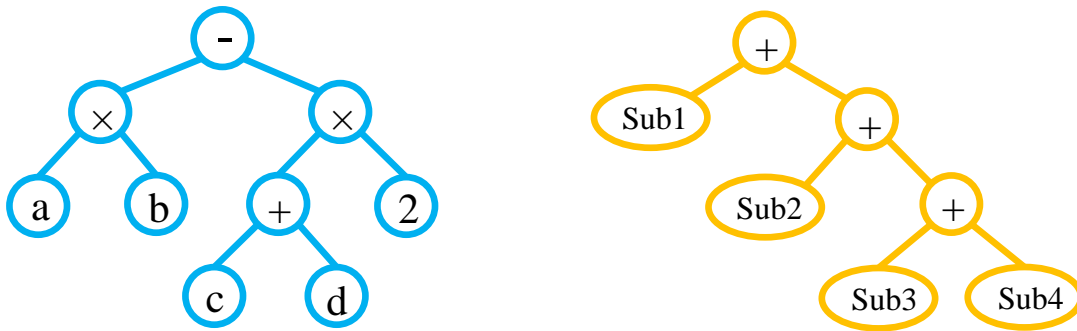
a) The expression tree of a sub-habitat Sub1   b) A habitat with four sub-habitats linked by addition

Fig. 2. Expression tree structure illustration of a sub-habitat and corresponding habitat.

The flowchart of BBP is shown in Fig. 3 and the main steps of this proposed metaheuristic programming are explained in detail below.
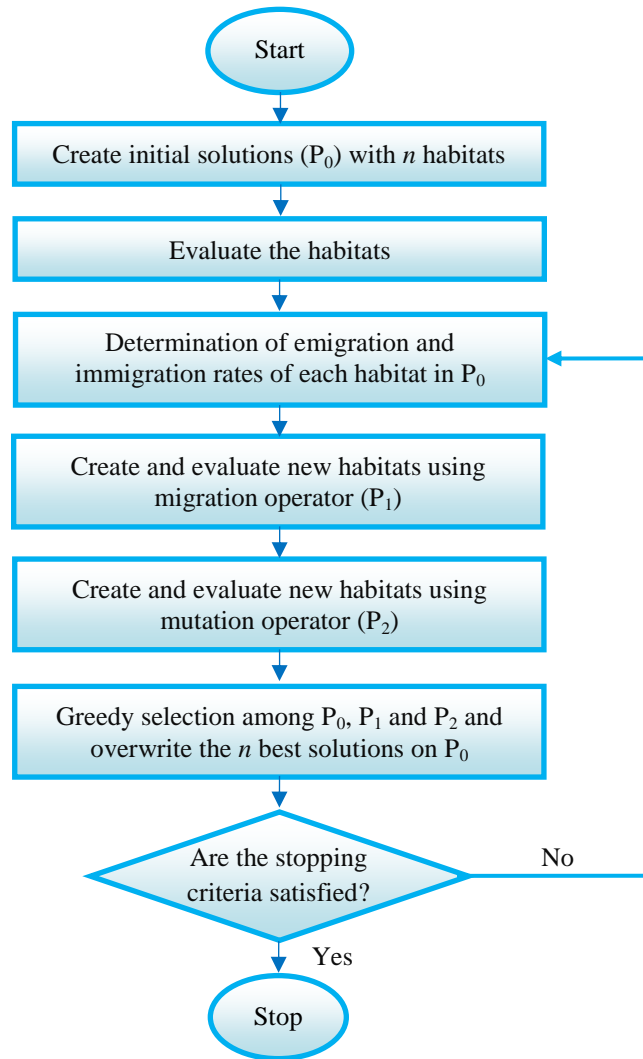
Fig. 3. The flowchart of BBP algorithm.

- **Create initial population (P_0):** It consists of n initial habitats that are generated with a randomized selection procedure. Each habitat consists of one or more sub-habitats and presents a possible solution of the regression problem. Aggregation of sub-habitats by summation operator constructs habitat which has mathematically an expression tree consisting of variables, functions and constants.
- **Evaluate the solutions:** The goal of BBP is to find a habitat that performs well for all patterns in the database with low error. In the BBP, habitat suitability index (HSI) is used for evaluating each solution. In the proposed algorithm, the term HSI is the root mean squared error (RMSE) defined in Eq. 3 below, which must be minimized. Habitat with a high HSI has a low RMSE and tends to have a large number of species. RMSE minimization results in "better" expressions over the generations. The best expression is chosen as the expression with greatest HSI or least RMSE.

- **Determination of emigration and immigration rates:** the immigration rate λ is assigned to control habitat immigration. The maximum immigration rate in a single habitat (*I*) occurs when there are no species in this habitat. As the number of species in a habitat increases, it will become crowded and, consequently, fewer species would be able to survive in this habitat and the immigration will subsequently decrease. Emigration rate μ is another attribute of a habitat in BBP that controls habitat emigration. If there are no species in a habitat, its emigration is null. As the number of species increases, species are capable to leave their habitat in order to explore other and maybe better residences. The maximum emigration rate (*E*) occurs in a single habitat when containing the maximum number of species it can support.

- **Create and evaluate new solutions using migration operator (P_1):** The migration operator is used to migrate species between two habitats according to their immigration and emigration rates. The migration from one habitat to another one is done by swapping a part of a sub-habitat of one habitat with a part of a sub-habitat of the other. The migration operator used for the BBP proceeds by the following steps:
  - Choose two habitats based on their immigration and emigration rates. The habitat with high HSI is more probable to be selected for emigration and the chance of habitat with low HSI being selected for immigration is high; indeed, the migration from a habitat with high HSI to a habitat with low HSI is more probable. The candidate habitats for emigration and immigration are named emigrated and immigrated habitats, respectively.
  - Select separately two random sub-habitats from the emigrated and immigrated habitats.
  - Choose separately two random subtrees from the above selected sub-habitats.
  - Migrate the selected subtree from the chosen sub-habitat of the emigrated habitat to the selected subtree from the chosen sub-habitat of the immigrated habitat. The resulting tree is a new habitat that its depth should be checked.

- The process of migration operator is shown, using two arbitrary simple expressions as selected sub-habitats of emigrated and immigrated habitats, in Fig. 4. After the new habitat was created, its HSI is evaluated and saved in migrated population P_1.
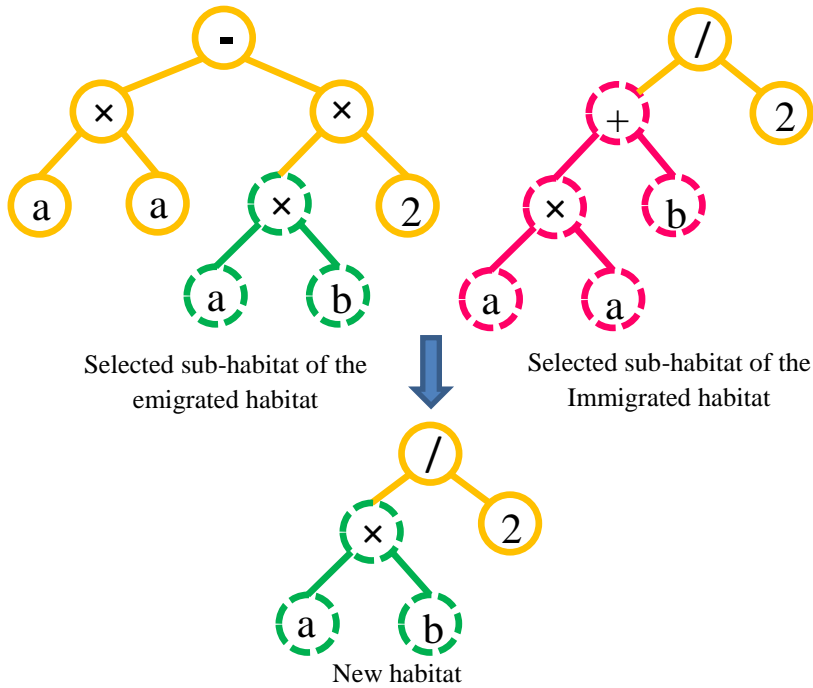
Fig. 4. Example of migration operator.

- **Create and evaluate new solutions using mutation operator (P_2)**: The mutation operator introduces random changes in the structures of the habitats in the population P_0. In this regard, a random sub-habitat from one random habitat is selected and a random point within its tree structure is chosen. Then, mutation operator removes whatever is currently at the selected point and whatever is below the selected point and inserts a randomly generated subtree at that point. This operator is controlled by a parameter that specifies the maximum size of tree depth for the newly created subtree that is to be inserted. This process is shown in Fig. 5, where an arbitrary simple sub-habitat from a random selected habitat is mutated by replacing one of its subtrees with a random tree. After applying the mutation operator, the performance of the created habitat is evaluated and saved in mutated population P_2.

9

Fig. 5. Example of mutation operator.

- **Greedy selection among P_0, P_1 and P_2 and overwrite the *n* best solutions on P_0:**

    In this section, the populations P_0, P_1 and P_2 are merged and the *n* best habitats based on greedy selection of habitats in the merged population are selected. Then, the old population P_0 is replaced with a new population.
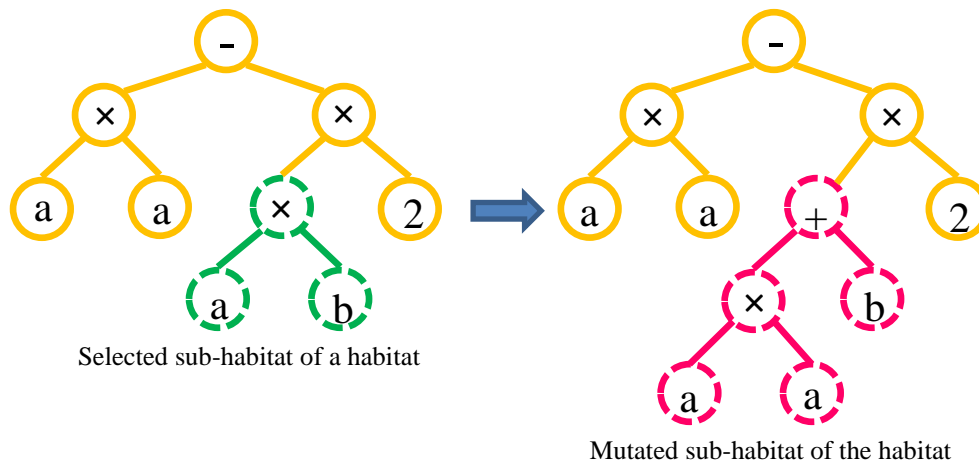
- **Investigation of the stopping criteria:**

    Termination is the criterion by which the BBP decides whether to continue searching or stop the search. Each of the enabled termination criterion is checked after each generation to see whether it is time to stop the process. Different types of stopping criteria may be implemented, for example generation number, time period, fitness threshold, the number of node evaluations, etc.

5. Modeling the shear capacity of FRP-RC beams

5.1. Experimental data

The model's success in predicting the shear capacity of FRP-RC beams depends on comprehensiveness of the training data. Availability of large variety of experimental data was required to develop the relationship between the effective parameters on shear capacity and its measured properties. Based on the previous research studies, the basic effective parameters that affecting the shear capacity of FRP-RC beams are the width of web (b_w), effective depth of beam (d), shear span to depth ratio (a/d), concrete compressive strength (f'_c), longitudinal reinforcement ratio (ρ_f) and elastic modulus of FRP bars (E_f) [35, 45-49]. An experimental database of 138 test specimens failed in shear was obtained from different previous investigations [31, 36, 45, 47, 49-65]. During the collection stage, specimens with shear span to depth ratios between 2.4 and 6.5 were included but deeper and slender beams were omitted from the database. In order to reduce the noise in the database collected, the output values of specimens with the same input values were averaged and included in database as a single entry. Of the 87 test specimens in the refined database, 77 were beams and the other 10 were one way slabs. All test specimens in the database have no transverse shear reinforcement and were simply supported tested under either one or two point loads acting symmetrically with respect to the centerline of the beam span as depicted schematically in Fig. 6. The limit values of input and output variables are listed in Table 2. Also, the complete list of data is given in Table A.1, where the name and the source of each specimen are referenced.

Table 2

Ranges of inputs and output variables in database.

Variables	Min	Max	Average	Standard deviation
b_w (mm)	89.00	1000.00	304.57	242.07
d (mm)	141.00	970	276.40	155.22
a/d	2.50	6.50	3.85	1.20
f'_c (MPa)	22.70	81.40	43.05	14.19
ρ_f (%)	0.25	3.02	1.24	0.62
E_f (GPa)	29.00	192.00	71.78	53.62
V_{cf} (KN)	9.80	220.70	71.78	53.62
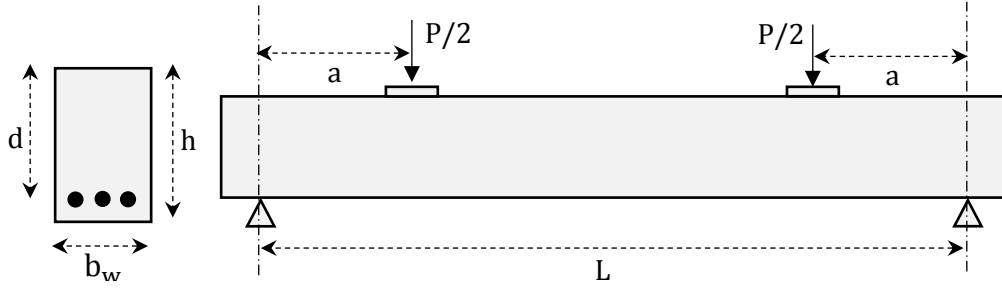
Fig. 6. Geometry of shear capacity test using two-point loading system (One-point loading system: a=L/2).

In order to investigate the generalization capability of the BBP model, the experimental database is divided into two sets, namely training and testing data sets. The formulation is based on the training sets and is further tested by test set values to measure its generalization capability. The patterns used in test and training sets are randomly selected. However, the distribution of each influencing parameters across its range in training data set was manually examined to ensure that it covers a good spread within the range considered. Of the 87 specimens in database, 70 specimens were taken for training process and the remaining 17 specimens were used for testing of the proposed model.

The scaling of the data samples is always recommended in system modeling. In this study, data samples were scaled in the range -1 and 1 using the following linear equation:

$$X_n = \frac{2(X - X_{min})}{X_{max} - X_{min}} - 1 \qquad (1)$$

where X_{min}, X_{max} and X_n denote the minimum, maximum and scaled value of the X data sample, respectively. It should be noted that any new input data should be normalized before simulated by the BBP and the corresponding predicted values should be un-normalized before use.

5.2. Performance measures

In order to evaluate the model results, it is important to define the criteria by which the performance of the model and its prediction accuracy are assessed. The best model was chosen on the basis of a multi-objective strategy as follows [66, 67]:

i. Selecting the simplest model, although this is not a predominant factor.
ii. Providing the best fitness value on the training data.
iii. Providing the best fitness value on the validation data.

The first objective can be controlled by the user through the parameter settings (e.g., tree depth or the number of habitats). For the other two objectives, the following objective function (OBJ) is used as a measure of how well the model predicted output agrees with the experimentally measured output. The selection of the best BBP model is based on the minimization of the objective function (OBJ) below [68]:

11

$$\text{OBJ} = \left(\frac{\text{No.}_{\text{Train}} - \text{No.}_{\text{Test}}}{\text{No.}_{\text{Train}} + \text{No.}_{\text{Test}}}\right)\frac{\text{RMSE}_{\text{Train}} + \text{MAE}_{\text{Train}}}{\text{R}_{\text{Train}} + 1} + \frac{2\text{No.}_{\text{Test}}}{\text{No.}_{\text{Train}} + \text{No.}_{\text{Test}}} \times \frac{\text{RMSE}_{\text{Test}} + \text{MAE}_{\text{Test}}}{\text{R}_{\text{Test}} + 1} \tag{2}$$

where $\text{No.}_{\text{Train}}$ and No._{Test} are the number of training and testing data, respectively. RMSE, MAE and R are, respectively, the root mean squared error, mean absolute error and correlation coefficient and calculated using the following equations [68]:

$$\text{RMSE} = \frac{\sqrt{\sum_{i=1}^{n}(h_i^2 - t_i^2)}}{n} \tag{3}$$

$$\text{MAE} = \frac{\sum_{i=1}^{n}|h_i - t_i|}{n} \tag{4}$$

$$R = \frac{\sum_{i=1}^{n}(h_i - \bar{h}_i)(t_i - \bar{t}_i)}{\sqrt{\sum_{i=1}^{n}(h_i - \bar{h}_i)^2 \sum_{i=1}^{n}(t_i - \bar{t}_i)^2}} \tag{5}$$

In which h_i and t_i are, respectively, actual and calculated outputs for ith output, $\bar{h}_i$ and $\bar{t}_i$ are the average of actual and predicted outputs, respectively, and n is the number of samples. The constructed objective function simultaneously takes into account the changes of R, RMSE and MAE. Higher R and lower RMSE, MAE values result in lowering OBJ, and hence indicate a more precise model. In addition, the above function considers the effects of different data divisions for the training and testing data sets [68]. Another statistical parameter, namely, mean absolute percentage error (MAPE) for training and testing data was also used as defined below:

$$\text{MAPE} = \frac{1}{n}\sum_{i=1}^{n}\frac{|h_i - t_i|}{t_i} \times 100 \tag{6}$$

5.3. Development of empirical models using BBP

Six input parameters, b_w, d, a/d, f'_c, ρ_f and E_f, were used to create the BBP model. The parameter selection affects the model generalization capacity of BBP. Several runs were conducted to come up with a parameterization of BBP that provided enough robustness and generalization for the prediction of shear capacity of FRP reinforced concrete elements. Table 3 presents the parameter settings for the BBP algorithm. As shown in this table, four basic arithmetic operators ($+$, $-$, $\times$, $/$) and basic mathematical functions ($\log(|x|)$, $|x|^y$, x^2, x^3, x^4, x^5, $\sqrt{|x|}$, $\sqrt[3]{|x|}$, $\sqrt[4]{|x|}$ and $\sqrt[5]{|x|}$) were utilized to get the optimum BBP model. In this problem, each habitat is a nonlinear formula for predicting the shear capacity of FRP-RC beams which is stated according to the above defined functions. The number of habitats in the population, that BBP will evolve, is set by the population size. Indeed, each population consists of different candidate formulas for predicting the shear capacity of FRP-RC beams. A run will take longer with a larger population size as more number of candidate formulas should be evaluated. The maximum generation sets the stopping criteria of a run. The proper number of population and generation depends on the number of possible solutions and complexity of problem. Three levels were set for the population size. The habitat architectures of the models evolved by BBP include initial tree size, maximum tree size and the number of sub-habitats. The initial tree size parameter sets the size of the candidate shear capacity formula in the first population at the start of each run and the maximum tree size parameter determines its complexity in the evolved model during each run.

The number of terms in the model is determined by the number of sub-habitats. Increasing the number of sub-habitats produces more complicated formula for shear capacity of FRP-RC beams and significantly increases the computational time. In the current modelling, three and two levels were considered for the maximum tree size and the number of sub-habitats, respectively. The addition linking function was used to link the mathematical terms encoded in each sub-habitat. Different combinations of the parameters are considered, namely three levels for the population size, three levels for the maximum tree size and two levels for the number of sub-habitats, giving a total of 18 different combinations. All of these combinations were tested and ten replications for each combination were carried out. Therefore, the overall number of BBP runs was equal to $18 \times 10 = 180$. Moreover, the total number of 540,000,000 candidate formulas for predicting the shear capacity of FRP-RC beams was evaluated. The success of the BBP algorithm usually increases with increasing the population size, maximum tree size and the number of sub-habitats. In this case, the complexity of the evolved functions and subsequently the shear capacity formula of FRP-RC beams increases and the speed of the algorithm decreases.

Table 3
The main parameters of BBP model.

Parameters	Values
Functions[*]	$+$, $-$, $\times$, $/$, $\log(|x|)$, $|x|^y$, x^2, x^3, x^4, x^5, $\sqrt{|x|}$, $\sqrt[3]{|x|}$, $\sqrt[4]{|x|}$, $\sqrt[5]{|x|}$
Population size	100-300-500
Maximum generation	10000
Selection	Tournament
Tournament size	3
Initial tree size	6
Maximum tree size	5-7-9
The number of sub-habitats	3-4
Constants	[-1,1]
Migration probability	0.90
Mutation probability	0.10
Probability of constant selection	0.2
Raw fitness	Root mean squared error

* x and y can be each of input variables.

6. Results and discussion

After running different BBP models, the final model was obtained. The population size, maximum tree size and the number of sub-habitats of the best BBP model are 500, 9 and 4, respectively. The formulation of the best BBP model for predicting the shear capacity of FRP-RC beams is presented in Table 4. The convergence rate of the best BBP model for training and testing data is also plotted in Fig. 7. As expected, the RMSE for both training and testing data significantly decreases in the initial generations and, then, the rate of error reduction becomes less. In addition, the mean error value of habitats in population decreases gradually and it becomes close to the error value of the best habitat in the final generations.

Table 4

The optimum BBP equations in LISP programming language format for predicting the shear capacity of FRP-RC beams (note: $F_1,..., F_{14}$ represent $+$, $-$, $\times$, $/$, $\log(|x|)$, $|x|^y$, x^2, x^3, x^4, x^5, $\sqrt{|x|}$, $\sqrt[3]{|x|}$, $\sqrt[4]{|x|}$ and $\sqrt[5]{|x|}$, respectively.).

Sub1 = $F_3(F_{13}(F_2(b_w,F_6(F_{13}(F_6(F_{11}(F_{12}(E_f)),F_7(F_2([-0.9129],\rho_f)))), F_7(F_2(F_2(E_f,\rho_f),F_3(F_6(\rho_f,b_w),F_4(\rho_f,b_w)))))))),$
$F_3(b_w,F_{12} (F_6(F_7(b_w), F_1(F_6(d,F_2(F_2(b_w,\rho_f),\rho_f)),F_1(\rho_f,F_4(F_8(E_f),F_2([0.3703], b_w))))))))))$

**Sub2** = $F_6(F_3(F_{13}(F_3(F_6(b_w,F_6(F_2([-0.9129],\rho_f),F_{10}(F_2([0.3703], b_w)))),$ $F_7(b_w))),$ $F_2(F_{13}(d),[-0.0258])),$
$F_1(F_{10}(F_{10}(d)),$ $F_4(F_4(F_{11}(F_{10}(d)),$ $F_6(F_6(F_{11}(E_f),$ $F_6(F_2(a/d,d),$ $F_3(E_f,E_f))),$ $F_6(F_2(b_w,[-0.3288]),$ $F_3(E_f,a/d)))),$
$F_6(F_{13}(F_1(F_6(F_{10}(d),b_w),$ $F_1(\rho_f,F_2(b_w,d)))),$ $F_1(F_6(F_3(F_9(f'_c,),$ $F_2(b_w,\rho_f)),F_2(F_3(b_w,d),\rho_f)),$ $F_1(F_4(F_8(E_f),[0.3703]),$
$F_8(E_f)))))))$

Sub3 = $F_3(d,F_{12}(F_3(F_{12}(F_1(F_8(E_f),$ $F_3(F_4([0.5331],d),$ $F_{11}(F_2(E_f,a/d))))),$ $F_{12}(F_6(F_6(F_{12}(F_9(b_w)),$ $F_6(F_1([-0.3287],E_f),$
$F_2(b_w,\rho_f))),$ $F_6(F_1(F_9([0.9072]),\rho_f),$ $F_5(d)))))))$

V_{cf} = $Sub_1 + Sub_2 + Sub_3$
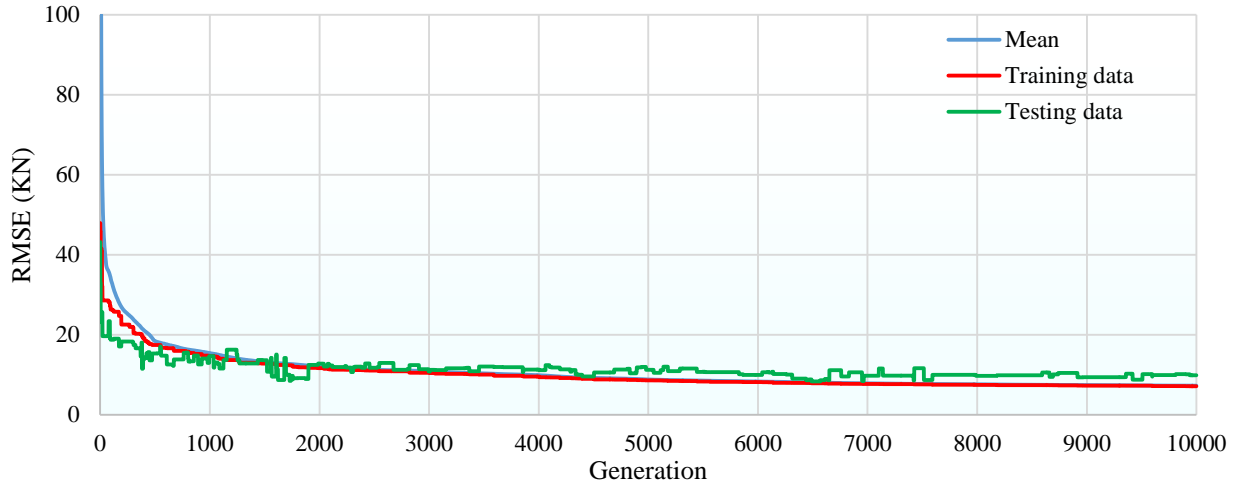
Fig. 7. Convergence graphic for training and testing data and mean value of RMSE in population.

The predicted shear capacity of FRP-RC beams versus experimental results for training and testing datasets is given in Fig. 8. The coefficient of the determination of the predicted vs. experimental values (according to the fit line equation as Predicted = a × Observed) and analysis of the residuals were calculated for training and testing data. According to the fit line equation in Fig. 8, it can be seen that the coefficient for the training and testing data is very close to 1, indicating that the proposed BBP model has successfully learnt the nonlinear model for the shear capacity prediction of FRP-RC beams. Fig. 9 shows a comparison between the experimental results and the estimates of shear capacity of FRP-RC beams obtained using the proposed BBP model. The test specimen number as listed in Table A.1 (Appendix A) is shown as the horizontal axis in Fig. 9. It can be seen that the results from BBP method are in good agreement with the experimental results.
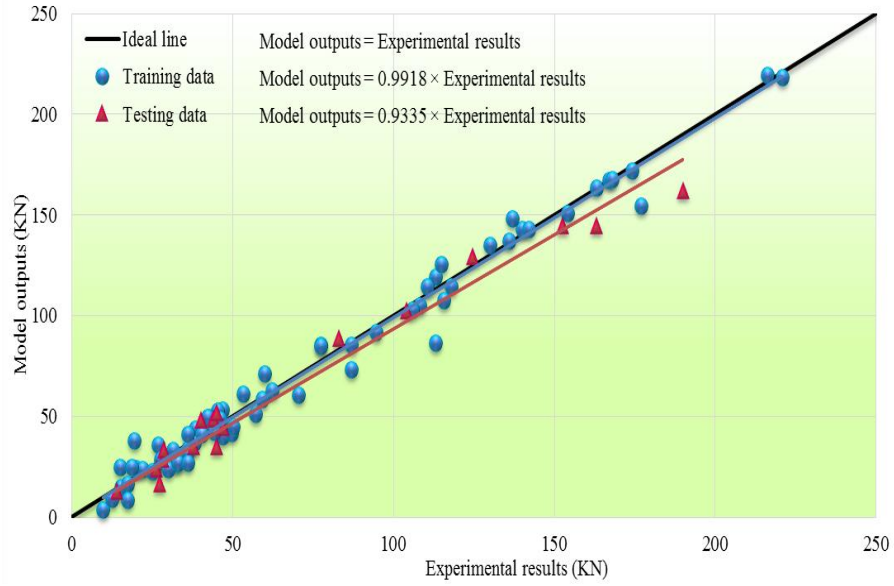
Fig. 8. BBP predictions versus experimental results for training and testing data
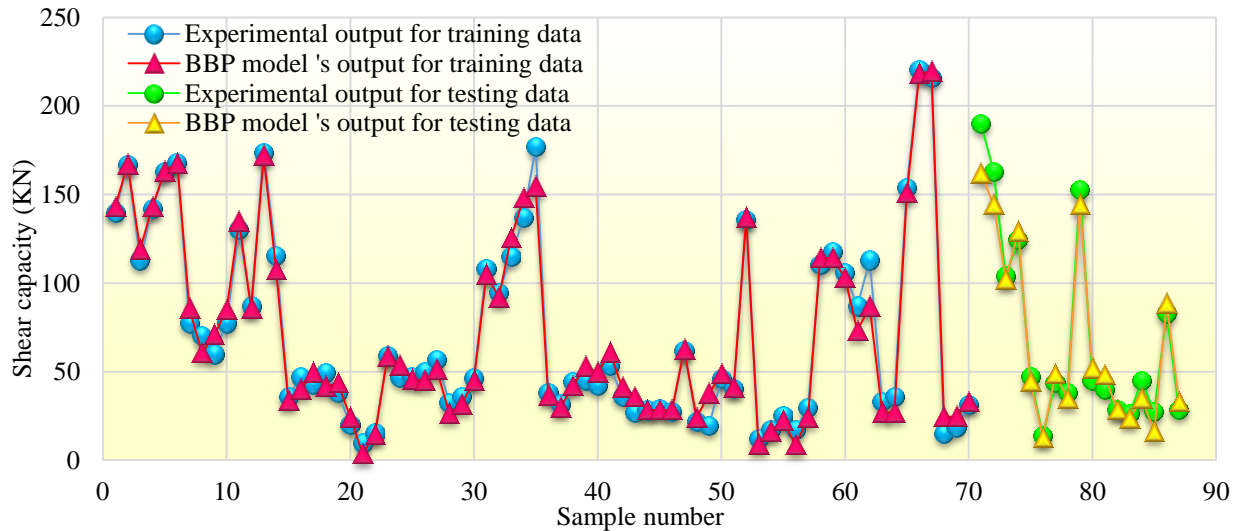
Fig. 9. Comparison between the experimental results and BBP predictions for training and testing data

The statistical parameters of training and testing data of the proposed BBP, Artificial Neural Network (ANN) model proposed by Bashir and Ashour [32], Gene Expression Programming (GEP) model proposed by Kara [37] and design equations are presented in Table 5. It is obvious from this table that BBP and ANN models present better predictions than GEP and other existing design equations. Table 5 also indicates that the shear capacity equations provided by ACI and ISIS overestimate the shear capacity of FRP-RC beams. Furthermore, the results demonstrate that the proposed BBP model is slightly better than ANN model in predicting the shear capacity of beams in the training dataset, whereas the performance of ANN is better than BBP model in predicting the experimental results in the testing dataset. Comparing the OBJ values that include the training and testing data simultaneously as defined by Eq. (2) for BBP and ANN models

15

indicates that the proposed BBP model is, overall, superior to ANN model. However, these comparisons are not conclusive as they are based on only comparison of statistical parameters for the ratio between the predicted and experimental shear capacities of limited test specimens.

Table 5
Statistical parameters of different shear capacity prediction models of FRP-RC beams.

Models	Data set	Statistical parameters				
		MAE	MAPE	RMSE	R	OBJ
BBP	Training	5.2424	12.5060	7.1646	0.9909	7.1558
	Testing	7.1801	11.7689	9.9081	0.9879	
ANN	Training	6.6148	13.2308	9.9999	0.9822	8.1070
	Testing	6.7363	11.5020	8.5369	0.9891	
GEP	Training	14.9203	18.8888	24.0608	0.9147	17.3414
	Testing	10.0889	12.3744	15.0286	0.9875	
ACI	Training	32.0737	44.4112	40.1363	0.9436	37.3790
	Testing	33.2925	47.2413	41.7989	0.9901	
CNR	Training	14.1129	25.7844	19.7705	0.9403	15.5142
	Testing	9.8217	18.0110	14.7504	0.9695	
ISIS	Training	21.8716	30.0845	30.9046	0.8952	27.4987
	Testing	21.8970	30.3112	30.4961	0.9437	

A qualitative study of the influencing parameters using the proposed BBP model was performed. All input parameters were set at the average value of the experimental specimens in the database while the chosen parameter to be studied was varied into the range of values specified in Table 2. In calculations, the average input parameters are taken as b_w=200 mm, d=300 mm, a/d=3.5, f_c'=40 MPa, ρ_f=1.5% and E_f=40 GPa. Fig. 10 presents the trend of the shear capacity predictions of FRP-RC beams to the variations of various design parameters, b_w, d, a/d, f_c', ρ_f, E_f. It can be clearly seen from these figures that the influence of different input parameters on the shear capacity of FRP-RC beams is different. However, the effect of b_w, d, ρ_f and E_f on the shear capacity of FRP-RC beams is very important. In general, the shear capacity continuously increases with the increase of b_w, d, ρ_f, f_c' and E_f and decreases due to increasing in a/d.
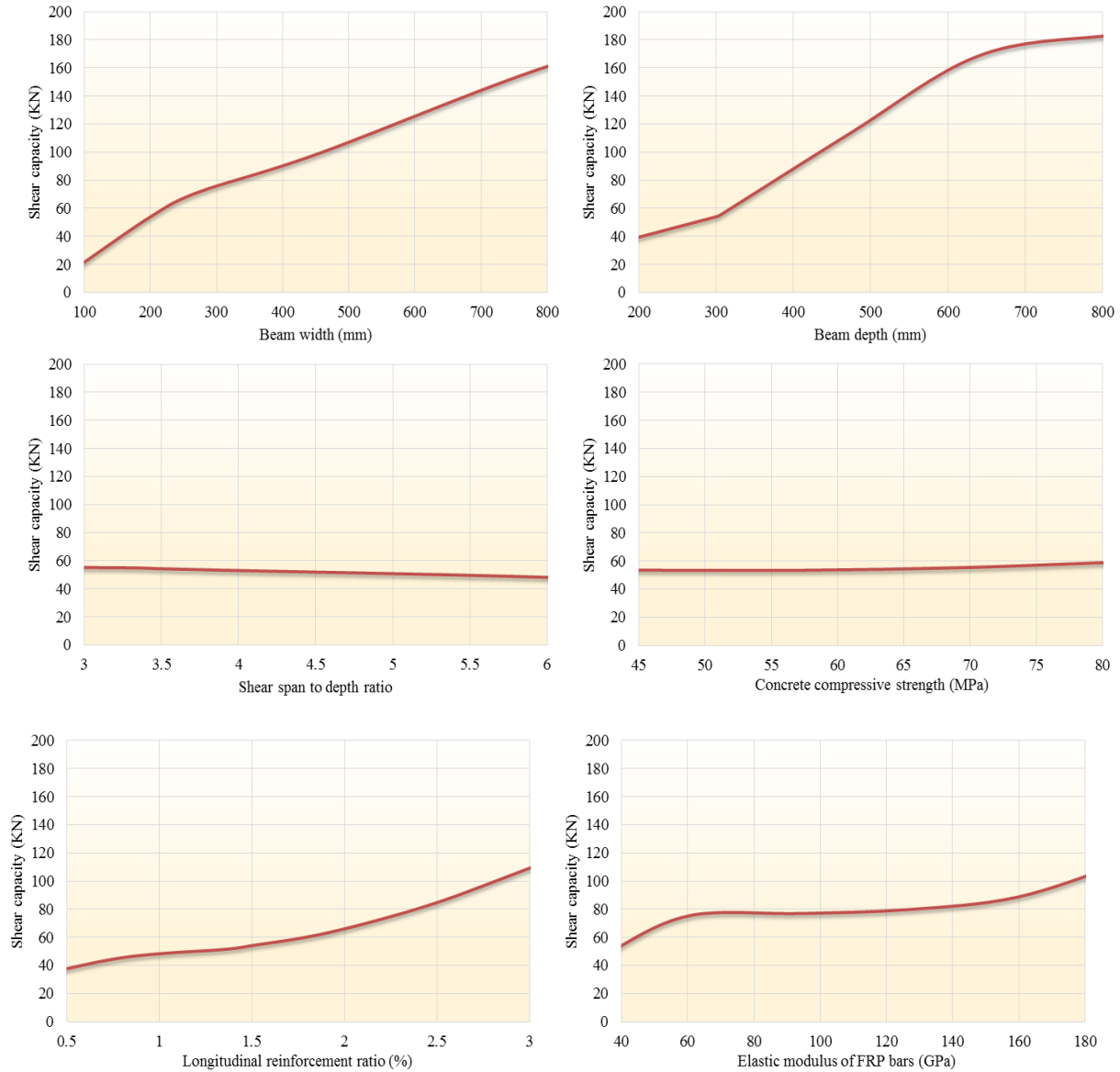
Fig. 10. Effect of different input parameters on the shear capacity of FRP-RC beams.

7. Conclusions

An empirical formulation using the Biogeographical-Based Programming (BBP) algorithm for predicting the shear capacity of FRP-RC beams based on test results available in the literature has been developed. The BBP model uses the web width (b_w), effective depth (d), shear span to depth ratio (a/d), concrete compressive strength (f_c'), longitudinal FRP reinforcement ratio (ρ_f) and elastic modulus of FRP bars (E_f) as the main parameters affecting the shear capacity. Different BBP models were executed and the best BBP model was chosen for further investigation and qualitative study. The final BBP model has population, sub-habitat and maximum tree sizes of 500, 3 and 9, respectively. Overall, the performance of the BBP model showed a slightly better comparison with experimental results than the artificial neural network (ANN), Genetic expression programming (GEP) and existing shear design equations. This study

has shown that the feasibility of the potential use of BBP model in predicting the shear capacity of FRP-RC beams. The proposed BBP algorithm has also correctly predicted the trend of different influencing parameters on the shear capacity of FRP-RC beams.

Appendix A

Table A.1. Experimental database used for training and testing the BBP model.

Row	b_w (mm)	d (mm)	a/d	f'_c (Mpa)	ρ (%)	E_f (GPa)	V_{cf} (KN)	ANN (KN)	GEP (KN)	BBP (KN)	References
					Training data						
1	1000.00	165.30	6.00	40.00	0.39	114.00	140.00	144.33	112.58	143.14	[50]
2	1000.00	165.30	6.00	40.00	0.78	114.00	167.00	165.35	141.85	166.06	
3	1000.00	162.10	6.20	40.00	0.86	40.00	113.00	114.14	100.99	118.51	
4	1000.00	159.00	6.30	40.00	1.70	40.00	142.00	137.86	124.10	143.10	
5	1000.00	159.00	6.30	40.00	2.44	40.00	163.00	166.33	139.98	163.32	
6	1000.00	154.10	6.50	40.00	2.63	40.00	168.00	168.00	138.62	167.80	
7	250.00	326.00	3.10	50.00	0.87	128.00	77.50	106.16	87.39	80.39	[45]
8	250.00	326.00	3.10	50.00	0.87	39.00	70.50	59.24	58.80	60.53	
9	250.00	326.00	3.10	44.60	1.22	42.00	60.00	74.07	64.94	70.64	
10	250.00	326.00	3.10	43.60	1.71	42.00	77.50	87.08	72.13	84.34	
11	250.00	326.00	3.10	63.00	1.71	135.00	130.00	138.30	120.35	135.18	[36]
12	250.00	326.00	3.10	63.00	1.71	42.00	87.00	88.78	81.55	84.91	
13	250.00	326.00	3.10	63.00	2.20	135.00	174.00	162.62	130.89	173.69	
14	250.00	326.00	3.10	63.00	2.20	42.00	115.50	106.94	88.69	109.12	
15	200.00	225.00	2.70	40.50	0.25	145.00	36.10	44.02	31.42	34.23	[51]
16	200.00	225.00	2.70	49.00	0.50	145.00	47.00	46.08	42.18	39.81	
17	200.00	225.00	2.70	40.50	0.88	145.00	42.70	47.44	47.79	45.57	
18	200.00	225.00	3.60	40.50	0.50	145.00	49.70	44.77	38.34	41.57	
19	200.00	225.00	4.20	40.50	0.50	145.00	38.50	44.77	37.69	43.62	
20	159.00	141.00	6.50	61.80	0.58	139.00	19.97	17.83	21.33	25.39	[52]
21	89.00	143.00	6.40	81.40	0.47	139.00	9.80	9.70	12.40	13.82	
22	121.00	141.00	6.50	81.40	0.76	139.00	15.40	17.11	19.48	14.66	
23	160.00	346.00	2.80	37.30	0.72	42.00	59.10	49.25	35.26	58.26	[53]
24	160.00	325.00	3.50	34.10	1.54	42.00	46.80	52.00	40.40	52.75	
25	130.00	310.00	3.10	37.30	0.72	120.00	47.50	60.13	36.01	44.30	
26	130.00	310.00	3.70	43.20	1.10	120.00	50.15	63.48	42.71	44.76	
27	130.00	310.00	3.70	34.10	1.54	120.00	57.10	54.38	44.15	51.49	
28	152.00	225.00	4.10	79.60	1.66	40.30	32.50	29.55	35.02	26.57	[54]
29	165.00	224.00	4.10	79.60	2.10	40.30	35.77	36.13	40.94	31.11	
30	203.00	224.00	4.10	79.60	2.56	40.30	46.40	49.89	53.80	45.94	
31	457.00	360.00	3.40	39.70	0.96	40.50	108.10	104.95	113.85	104.68	[49]
32	457.00	360.00	3.40	39.70	0.96	37.60	94.70	100.74	111.06	91.76	
33	457.00	360.00	3.40	40.30	0.96	47.10	114.80	113.66	120.32	125.23	
34	457.00	360.00	3.40	42.30	1.92	40.50	137.00	150.55	146.50	148.24	
35	457.00	360.00	3.40	42.60	1.92	47.10	177.00	160.91	154.43	154.92	
36	229.00	225.00	4.10	36.30	1.11	40.30	38.10	37.72	35.52	36.64	[55]
37	178.00	225.00	4.10	36.30	1.42	40.30	31.73	29.38	29.97	29.50	
38	229.00	225.00	4.10	36.30	1.66	40.30	44.43	41.14	40.62	41.88	
39	279.00	225.00	4.10	36.30	1.81	40.30	45.27	53.89	50.93	52.82	
40	229.00	224.00	4.10	36.30	2.27	40.30	42.20	46.37	44.88	49.45	
41	178.00	279.00	2.70	24.10	2.30	40.00	53.40	56.81	39.78	60.94	[56]
42	178.00	287.00	2.60	24.10	0.77	40.00	36.10	35.74	28.53	41.45	
43	305.00	157.50	4.50	28.60	0.73	40.00	26.80	33.09	26.26	35.70	[47]
44	305.00	157.50	5.80	30.10	0.73	40.00	28.30	27.48	25.97	30.54	

45	305.00	157.50	5.80	27.00	0.73	40.00	29.20	28.35	25.04	30.49	
46	305.00	157.50	5.80	30.80	0.73	40.00	27.60	27.33	26.16	30.54	
47	200.00	260.00	2.70	34.70	1.30	130.00	62.20	61.58	57.61	61.85	[57]
48	150.00	210.00	3.70	32.90	1.31	45.00	22.00	22.92	23.30	23.62	[58]
49	254.00	222.00	3.20	39.00	1.55	34.00	19.50	45.35	43.22	37.56	[59]
50	150.00	250.00	3.00	34.30	3.02	105.00	46.00	51.69	50.45	47.74	[60]
51	150.00	250.00	3.00	34.30	2.27	105.00	40.50	44.02	45.87	39.88	
52	450.00	970.00	3.10	40.00	0.46	40.00	136.00	140.21	238.41	136.53	[61]
53	150.00	171.00	3.90	34.00	0.45	38.00	12.50	11.36	12.62	8.85	[62]
54	150.00	218.00	3.10	34.00	0.71	32.00	17.50	14.58	18.15	16.44	
55	150.00	268.00	2.50	34.00	0.86	32.00	25.00	26.32	24.36	22.44	
56	150.00	168.00	4.00	59.00	1.39	32.00	17.50	9.26	20.44	8.50	
57	150.00	268.00	2.50	59.00	1.15	32.00	30.00	32.97	32.25	23.85	
58	200.00	325.00	3.20	44.60	0.70	137.00	110.50	87.01	63.60	113.15	[31]
59	200.00	325.00	3.20	45.00	0.70	137.00	118.00	87.41	63.79	113.14	
60	200.00	325.00	3.20	46.90	0.90	192.00	106.00	107.07	78.71	102.93	
61	200.00	325.00	3.20	46.90	0.90	58.00	87.00	71.31	52.81	73.02	
62	250.00	265.00	3.10	34.10	1.90	56.00	113.00	76.87	61.58	87.13	[63]
63	300.00	150.00	4.00	22.70	1.30	29.00	33.00	28.70	25.12	28.15	[64]
64	300.00	150.00	4.00	27.80	1.80	29.00	36.00	32.73	29.96	27.66	
65	457.00	883.00	3.10	29.50	0.59	40.70	154.10	157.24	217.61	151.93	[65]
66	457.00	880.00	3.10	29.50	1.18	40.70	220.70	216.37	273.25	217.07	
67	456.00	880.00	3.10	30.70	1.18	41.40	216.20	216.20	277.87	218.17	
68	114.00	294.00	3.10	59.70	0.59	40.80	15.20	25.33	22.88	24.54	
69	114.00	294.00	3.10	32.10	0.59	40.80	18.70	26.34	18.61	24.56	
70	229.00	147.00	3.10	32.10	0.59	40.80	31.55	23.90	18.69	33.01	
Testing data											
1	1000.00	160.50	6.20	40.00	1.18	114.00	190.00	180.95	157.53	160.72	[50]
2	1000.00	162.10	6.20	40.00	1.71	40.00	163.00	141.74	126.99	144.33	
3	250.00	326.00	3.10	44.60	1.24	134.00	104.00	115.56	96.12	101.01	[45]
4	250.00	326.00	3.10	43.60	1.72	134.00	124.50	127.04	106.39	129.75	
5	200.00	225.00	2.70	40.50	0.63	145.00	47.20	44.53	42.76	43.72	[51]
6	127.00	143.00	6.40	60.30	0.33	139.00	13.97	14.55	14.23	13.21	[52]
7	160.00	346.00	3.30	43.20	1.10	42.00	44.10	55.82	41.87	48.44	[53]
8	203.00	225.00	4.10	79.60	1.25	40.30	38.03	33.65	42.56	35.98	[54]
9	457.00	360.00	3.40	42.50	1.92	37.60	152.60	145.33	143.14	144.59	[49]
10	254.00	224.00	4.10	36.30	2.05	40.30	45.10	50.11	48.12	51.72	[55]
11	178.00	287.00	2.60	24.10	1.34	40.00	40.10	42.21	34.32	48.44	[56]
12	305.00	157.50	5.80	28.20	0.73	40.00	28.50	27.94	25.41	30.51	[47]
13	150.00	210.00	3.70	38.10	1.31	45.00	26.50	24.31	24.47	23.51	[58]
14	150.00	250.00	3.00	34.30	1.51	105.00	45.00	40.54	40.04	33.81	[60]
15	150.00	218.00	3.10	59.00	1.06	32.00	27.50	19.93	24.93	16.35	[62]
16	250.00	265.00	3.10	22.90	1.90	56.00	83.00	70.94	53.93	89.46	[63]
17	229.00	147.00	3.10	59.70	0.59	40.80	28.60	19.07	22.98	33.01	[65]

8. References

[1] American Concrete Institute (ACI) Committee 440. Report on fiber-reinforced polymer (FRP) reinforcement concrete structures. ACI 440R-07. Farmington Hills (MI): American Concrete Institute; 2007. P. 100.
[2] Fédération Internationale du Béton (fib). FRP reinforcement in RC structures. Task Group 9.3, Lausanne, Switzerland; 2007.

[3] Kassem C, Farghaly AS, Benmokrane B. Evaluation of flexural behavior and serviceability performance of concrete beams reinforced with FRP bars. J Compos Constr, ASCE 2011;15(5):682-95.

[4] El-Sayed A, Soudki K. Evaluation of shear design equations of concrete beams with FRP reinforcement. J Compos Constr, ASCE 2011;15(1):9-20.

[5] Tanarslan HM, Secer M, Kumanlioglu A. An approach for estimating the capacity of RC beams strengthened in shear with FRP reinforcements using artificial neural networks. Constr Build Mater 2012;30:556-68.

[6] Yu L, Francois R, Dang VH, L-Hostic V, Gagne R. Distribution of corrosion and pitting factor of steel in corroded RC beams. Constr Build Mater 2015;95:384-92.

[7] Tondolo F. Bond behavior with reinforcement corrosion. Constr Build Mater 2015;93:926-32.

[8] Kara IF, Ashour A. Flexural performance of FRP reinforced concrete beams. Comput Struct 2012;94(5):1616-25.

[9] Yost JR, Gross SP, Dinehart DW. Effective Moment of Inertia for Glass Fiber-Reinforced Polymer-Reinforced Concrete Beams. ACI Struct J 2003;100(6):732-39.

[10] Mari A, Cladera A, Oller E, Bairan J. Shear design of FRP reinforced concrete beams without transverse reinforcement. J Compos: Part B 2014;57:228-41.

[11] Kara I, Ashour A, Dundar C. Deflection of concrete structures reinforced with FRP bars. J Compos: Part B 2013;44(1):375-84.

[12] Tomlinson D, Fam A. Performance of concrete beams reinforced with basalt FRP for flexure and shear.J Compos Constr, ASCE; 2014, <http://dx.doi.org/10.1061/(ASCE)CC.1943-5614.0000491>.

[13] Razaqpur G, Spadea S. Shear strength of FRP reinforced concrete members with stirrups. J Compos Constr, ASCE 2015;19(1):1-15.

[14] Perera R, Arteaga A. De-Diego A. Artificial intelligence techniques for prediction of the capacity of RC beams strengthened in shear with external FRP reinforcement. Compos Struct 2010;92(5):1169-75.

[15] Schmidt MD, Lipson H. Co-evolving fitness predictors for accelerating and reducing evaluations, in: Genetic Programming Theory and Practice IV. Genet Evol Comput 2006;5:113-20.

[16] Karaboga D, Ozturk C, Karaboga N, Gorkemli B. Artificial bee colony programming for symbolic regression. Inform Sciences 2012;209:1-15.

[17] Koza JR, Genetic Programming: On the Programming of Computers by Means of Natural Selection, MIT Press, Cambridge, MA, USA, 1992.

[18] Musilek P, Lau A, Reformat M, Wyard-Scott L. Immune programming. Inform Sciences 2006;176(8):972-02.

[19] Shirakawa S, Ogino S, Nagao T. Dynamic ant programming for automatic construction of programs. IEEJ T Electr Elector 2008;3(5):540-48.

[20] Gan Z, Chow TWS, Chau WN. Clone selection programming and its application to symbolic regression. Expert Syst Appl 2009;36(2-2):3996-05.

[21] Simon D. Biogeography-based optimization. IEEE Trans Evol Comput 2008;12:702-13.

[22] Gong W, Cai Z, Ling C. DE/BBO: a hybrid differential evolution with biogeography based optimization for global numerical optimization. Soft Comput 2011;15(4):645-65.

[23] Ma H. An analysis of the equilibrium of migration models for biogeography-based optimization. Inform Sciences 2010;176(8):3444-64.

[24] Ma H, Simon D. Blended biogeography-based optimization for constrained optimization. Eng Appl Artif Intel 2011;24(3):517-25.

[25] Simon D, Ergezer M, Du D, Rarick R. Markov models for biogeography-based optimization. IEEE Trans Syst Man Cybern B Cybern 2011;41(1):299-06.

[26] Wang Y, Yang Y. Particle swarm optimization with preference order ranking for multi-objective optimization. Inform Sciences 2009;179(12):1944-59.

[27] Ma H, Simon D, Fei M, Shu X, Chen Z. Hybrid biogeography-based evolutionary algorithms. Eng Appl Artif Intel 2014;30:213-24.

[28] Boussaid I, Chatterjee A, Siarry P, Ahmed-Nacer M. Biogeography-based optimization for constrained optimization problems. Comput Oper Res 2012;39(12):3293-04.

[29] Xiong G, Shi D, Duan X. Enhancing the performance of biogeography-based optimization using polyphyletic migration operator and orthogonal learning. Comput Oper Res 2014;41:125-39.

[30] Li X, Wang J, Zhou J, Yin M. A perturb biogeography based optimization with mutation for global numerical optimization. Appl Math Comput 2011; 218(2):598-09.

[31] Kundra H, Kaur A, Panchal V. An integrated approach to biogeography based optimization with case based reasoning for retrieving groundwater possibility. In: 8th Annual Asian Conference and Exhibition on Geospatial Information, Technology and Applications, Singapore, August; 2009.

[32] Rarick R, Simon D, Villaseca F, Vyakaranam B. Biogeography-based optimization and the solution of the power flow problem. In: Proceedings of the IEEE Conference on Systems, Man, and Cybernetics, San Antonio, TX, October; 2009. p.1029-34.

[33] Japan Society of Civil Engineers, JSCE. Recommendation for design and construction of concrete structures using continuous fiber reinforcing materials. In: Machida A, editor. Concrete engineering series, vol. 23. Tokyo (Japan); 1997. p. 325.

[34] British Institution of Structural Engineers (BISE). Interim guidance on the design of reinforced concrete structures using fiber composite reinforcement, IStructE, SETO Ltd., London; 1999.

[35] CNR-DT 203. Guide for the design and construction of concrete structures reinforced with fiber-reinforced polymer bars. Rome, Italy: National Research Council; 2006.

[36] ISIS Canada. Reinforcing concrete structures with fiber reinforced polymers, ISISM03-07, Canadian network of centers of excellence on intelligent sensing for innovative structures. Manitoba: University of Winnipeg; 2007. p. 151.

[37] Tottori S, Wakui H. Shear capacity of RC and PC beams using FRP reinforcement. In: Fiber-reinforced-plastic reinforcement for concrete structures, SP-138. Detroit: American Concrete Institute; 1993. p. 615-32.

[38] Bashir R, Ashour A. Neural network modelling for shear strength of concrete members reinforced with FRP bars. J Compos: Part B 2012;43(8):3198-07.

[39] American Concrete Institute (ACI) Committee 440. Guide for the design and construction of structural concrete reinforced with FRP Bars. ACI 440.1R-06. Farmington Hills (MI): American Concrete Institute; 2006. p. 44.

[40] CAN/CSA S806-02. Design and construction of building components with fibre reinforced polymers. Canadian standards association, Rexdale, Ontario; 2002. p. 177.

[41] Razaqpur AG, Isgor OB. Proposed shear design method for FRP reinforced concrete members without stirrups. ACI Struct J 2006;103(1):93-02.

[42] El-Sayed AK, El-Salakawy E, Benmokrane B. Shear capacity of high- strength concrete beams reinforced with FRP bars. ACI Struct J 2006;103(3):383-89.

[43] Kara IF. Prediction of shear strength of FRP-reinforced concrete beams without stirrups based on genetic programming. Adv Eng Softw 2011;42(6):295-04.

[44] Nasrollahzadeh K, Basiri MM. Prediction of shear strength of FRP reinforced concrete beams using fuzzy inference system. Expert Syst Appl 2014;41(4-1):1006-20.

[45] Lee S, Lee C. Prediction of shear strength of FRP-reinforced concrete flexural members without stirrups using artificial neural networks. Eng Struct 2014;61(1):99-12.

[46] MacArthur R, Wilson E. The theory of biogeography, Princeton University Press, Princeton, New Jersey; 1967.

[47] Martiny J et al. Microbial biogeography: putting microorganisms on the map. Nature 2006;4(2):102-12.

[48] Whittaker R. Island biogeography. Oxford University Press, Oxford, UK; 1998.

[49] Gua W, Wang L, Wu Q. An analysis of the migration rates for biogeography-based optimization. Informa Sciences 2014;254(1):111-40.

[50] Ma H, Simon D, Fei M, Xie Z. Variations of biogeography-based optimization and Markov analysis. Inform Sciences 2013;220:492-06.

[51] El-Sayed AK, El-Salakawy EF, Benmokrane B. Shear strength of FRP-reinforced concrete beams without transverse reinforcement. ACI Struct J 2006;103(2):235-43

[52] El-Salakawy E, Benmokrane B. Serviceability of concrete bridge deck slabs reinforced with fiber-reinforced polymer composite bars. ACI Struct J 2004;101(5):727-36.

[53] Deitz DH, Harik IE, Gesund H. One-way slabs reinforced with glass fiber reinforced polymer reinforcing bars, fiber reinforced polymer reinforcemnet for reinforced concrete structures. In: Dolan CW, et al., editors., Proceedings of the 4-th international conference, SP-188. Farmington Hills, Mich: American Concrete Institute; 1999. p. 279-86.

[54] Michaluk R, Rizkalla S, Tadros G, Benmokrane B. Flexural behavior of one-way concrete slabs reinforced by fiber reinforced plastic reinforcement. ACI Struct J 1998;95(3):353-65.

[55] Tureyen AK, Frosch RJ. Shear tests of FRP-reinforced concrete beams without stirrups. ACI Struct J 2002;99(4):427-34.

[56] El-Sayed AK, El-Salakawy E, Benmokrane B. Shear strength of one way concrete slabs reinforced with FRP composite bars. J Compos Constr, ASCE 2005;9(2):147-57.

[57] Razaqpur AG, Isgor BO, Greenaway S, Selley A. Concrete contribution to the shear resistance of fiber reinforced polymer reinforced concrete members. J Compos Constr, ASCE 2004;8(5):452-60.

[58] Gross SP, Dinehart DW, Yost JR, Theisz PM. Experimental tests of high-strength concrete beams reinforced with CFRP bars. In: Proceedings of the 4th international conference on advanced composite materials in bridges and structures (ACMBS-4), Calgary, Alberta, Canada, July 20-23; 2004. p. 8.

[59] Tariq M, Newhook JP. Shear testing of FRP reinforced Concrete without transverse reinforcement. In: Proceedings of CSCE 2003-anuual conference, Moncton, NB, Canada; 2003. p. 10.

[60] Gross SP, Yost JR, Dinehart DW, Svensen E, Liu N. Shear strength of normal and high strength concrete beams reinforced with GFRP reinforcing bars. In: Proc.

[61] Yost JR, Gross SP, Dinehart DW. Shear strength of normal strength concrete beams reinforced with deformed GFRP bars. J Compos Constr, ASCE 2001;5(4):263-75.

[62] Alkhrdaji T, Wideman M, Belarbi A, Nanni A. Shear strength of GFRP RC beams and slabs. In: Proceedings of the international conference, composites in construction-CCC 2001, Porto/Portugal; 2001. p. 409-14.

[63] Mizukawa Y, Sato Y, Ueda T, Kakuta Y. A study on shear fatigue behavior of concrete beams with FRP rods. In: Proceedings of the third international symposium on non-metallic (FRP) reinforcement for concrete structures (FRPRCS-3), vol. 2. Sapporo (Japan): Japan Concrete Institute; 1997. p. 309-16.

[64] Duranovic N, Pilakoutas K, Waldron P. Tests on concrete beams reinforced with glass fibre reinforced plastic bars. In: Proceedings of the third international symposium on non-metallic (FRP) reinforcement for concrete structures (FRPRCS-3), vol. 2. Sapporo (Japan): Japan Concrete Institute; 1997. p. 479-86.

[65] Swamy N, Aburawi M. Structural implications of using GFRP bars as concrete reinforcement. In: Proceedings of the third international symposium on nonmetallic (FRP) reinforcement for concrete structures (FRPRCS-3), vol. 2. Sapporo (Japan): Japan Concrete Institute; 1997. p. 503-10.

[66] Zhao W, Mayama K, Suzuki H. Shear behaviour of concrete beams reinforced by FRP rods as longitudinal and shear reinforcement. In: Proceedings of the second international RILEM symposium on non-metallic (FRP) reinforcement.

[67] Lubell A, Sherwrvod T, Bents E, Collins MP. Safe shear design of large wide beams. Concr Int 2004;26(1):67-79.

[68] Ashour AF. Flexural and shear capacities of concrete beams reinforced with GFRP bars. Constr Build Mater 2005;20(10):1005-15.

[69] Nagasaka T, Fukuyama H, Tanigaki M. Shear performance of concrete beams reinforced with FRP stirrups. In: Nanni A, Dolan C, editors. ACI SP-138. Detroit, Mich: American Concrete Institute; 1993. p. 789-811.

[70] Nakamura H, Higai T. Evaluation of shear strength of concrete beams reinforced with FRP, concrete library international. Proc Jpn Soc Civil Eng 1995;26:111-23.

[71] Matta F, Nanni A, Hernandez TM, Benmokrane B. Scaling of strength of FRP reinforced concrete beams without shear reinforcement. In: Fourth international conference on FRP composites in civil engineering (CICE2008), Zurich, Switzerland; 2008. p. 6.

[72] Gandomi AH, Alavi AH, Yun GJ. Nonlinear modeling of shear strength of SFRCbeams using linear genetic programming. Struct Eng Mech 2011;38 (1):1-25.

[73] Gandomi AH, Alavi AH, Mousavi M, Tabatabaei SM. A hybrid computational approach to derive new ground-motion attenuation models. Eng Appl Artif Intell 2011;24(4):717-32.

[74] Gandomi AH, Yun GJ, Alavi AH. An evolutionary approach for modeling of shear strength of RC deep beams. Mater Struct 2013;46(12):2109-19.